Tensor Asymmetry A_{zz} in the $x > 1$ Region

A Proposal to Jefferson Lab PAC 42

E. Long, [†] [‡] K. Slifer,[†] P. Solvignon[†]
University of New Hampshire, Durham, NH 03861

D. Higinbotham[†]
Thomas Jefferson National Accelerator Facility, Newport News, VA 23606

[†]Spokesperson
[‡]Contact: ellie@jlab.org

Abstract

The tensor-polarized target asymmetry, A_{zz}, which is used to extract b_1 in the DIS region through the D(e, e')X channel, can be used to extract information on nucleon-nucleon interactions in the quasi-elastic region. The reaction is unique in that it can probe color transparency, which has never been explored at Jefferson Lab, and improve understanding of the deuteron wave function and particularly probe how short range correlations arise from proton-neutron interactions.

In the quasi-elastic region, A_{zz} was first calculated in 1988 by Frankfurt and Strikman, using the Hamada-Johnstone and Reid soft-core wave functions [1]. Recent calculations by M. Sargsian revisit A_{zz} in the $x > 1$ range using virtual-nucleon and light-cone methods, which differ by up to a factor of two [2].

An experimental determination of A_{zz} could be performed utilizing equipment identical for E13-12-011 at five different Q^2 values over the course of 24 days, with [NUMBER] additional days of commissioning. The measurements are less sensitive to the target polarization than E13-12-011, such that this experiment could be used to prove that the condition of 30% in-beam polarization is met for E13-12-011.

Contents

	$\overline{x}$	$\overline{Q^2}$ (GeV^2)	$\overline{W}$ (GeV)	P_0 (GeV)	θ (deg.)	Rates (kHz)	PAC Time (days)
HMS	0.90	1.3	1.01	5.83	10.55	0.88	14
SHMS	1.30	1.3	0.76	6.07	10.34	0.43	14

Table 1: Summary of the kinematics and physics rates using the Hall C spectrometers.

1 Quotes (To be removed)

"The most direct evidence for tensor correlations in nuclei comes from measurements of the deuteron structure functions and tensor polarization by elastic electron scattering [3]. In essence, these measurements have mapped out the Fourier transforms of the charge densitites of the deuteron in states with spin projections ± 1 and 0, showing that they are very different." -R. Schiavilla, et al. [4]

2 Background and Motivation

The deuteron is the simplest nuclear system, and in many ways it is as important to understanding bound states in QCD as the hydrogen atom was to understanding bound systems in QED. Unlike it's atomic analogue, our understanding of the deuteron remains unsatisfying both experimentally and theoretically.

Through electron scattering on tensor-polarized deuterons, the S- and D-wave states can be disentangled, leading to a fuller understanding of the repulsive nucleon core.

Understanding the nucleon-nucleon potential of the deuteron is essential for understanding short-range correlations. To resolve the short-range structure of nuclei on the level of nucleon and hadronic constituents, we need processes that transfer to the nucleon constituents both energy and momentum larger than the scale of the NN short range correlations. By scanning over a large range of Q^2, we can measure how these processes begin to dominate the tensor asymmetry A_{zz}.

2.1 Tensor Structure of the Deuteron

2.2 Quasi-Elastic and $x > 1$ Scattering from Spin-1 Targets

2.3 The Tensor Asymmetry A_{zz}

3 The Proposed Experiment

We will measure the tensor asymmetry $A_{zz}$for $0.80 < x < 1.75$, $1.0\,(\text{GeV}/c)^2 < Q^2 < 1.9\,(\text{GeV}/c)^2$ and $0.59 < W < 1.09$ GeV. Fig. 1 shows the planned kinematic coverage utilizing the Hall C HMS and SHMS spectrometers at forward angle.

$\overline{x}$	$\overline{Q^2}$ (GeV^2)	$\overline{W}$ (GeV)	f_{dil}	δA_{zz}^{stat} $\times 10^{-2}$
0.80	1.30	1.09	0.177	0.62
0.90	1.30	1.01	0.293	0.37
1.00	1.30	0.94	0.512	0.20
1.10	1.30	0.88	0.346	0.41
1.20	1.30	0.83	0.180	1.10
1.30	1.30	0.78	0.108	2.38
1.40	1.30	0.73	0.071	4.74
1.55	1.30	0.67	0.046	7.02
1.75	1.30	0.59	0.034	13.8

Table 2: Summary of the expected statistical uncertainty after combining overlapping x-bins. Values represent the statistics weighted average of all events that satisfy our kinematic cuts.

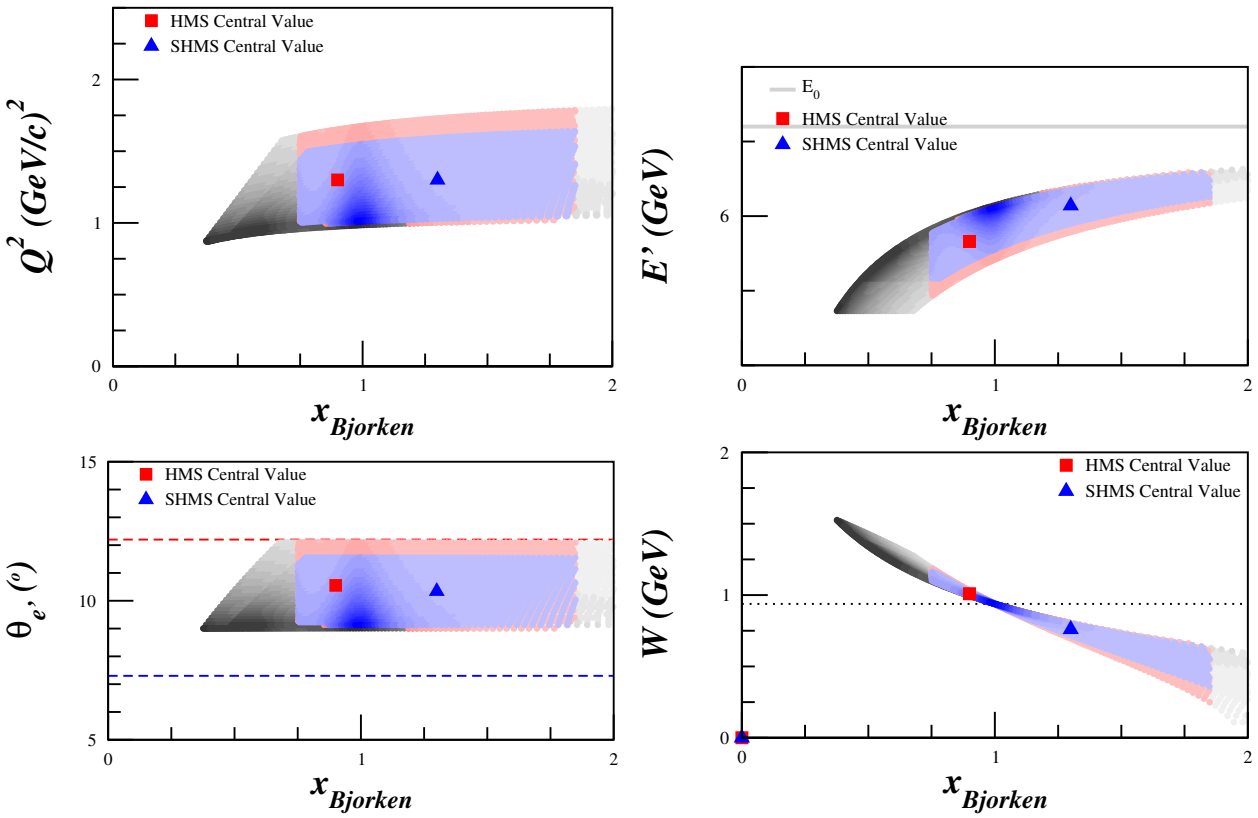

Figure 1: Kinematic coverage. The grey settings are not included in our rates estimates since they fall outside of $0.80 < x < 1.75$. The highlighted represent the central value of the spectrometer setting, which are not the statistics weighted average of the distribution. The shading represents areas with greater statistics.

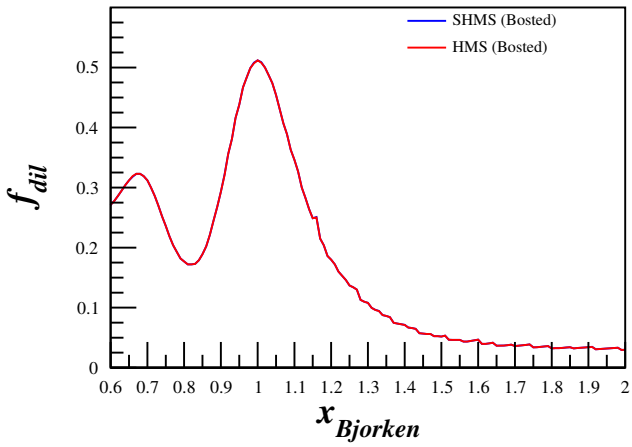

Figure 2: Projected dilution fraction covering the entire x range to be measured using the Bosted fits [5] for the SHMS and HMS. In the kinematics used, both dilution factors overlap.

The polarized LiD target is discussed in section **??**. The magnetic field of the target will be held constant along the beamline at all times, while the target state is alternated between a polarized and unpolarized state. The tensor polarization and packing fraction used in the rates estimate are 30% and 0.65 , respectively. The packing fraction changes with x in the range of this measurement as shown in Fig. 2. With an incident electron beam current of 115 nA, the expected deuteron luminosity is 1.57×10^{35} / cm^2·s^1. The momentum bite and the acceptance were assumed to be $\Delta P = \pm 8\%$ and $\Delta\Omega = 5.6$ msr for the HMS, and $\Delta P = ^{+20\%}_{-8\%}$ and $\Delta\Omega = 4.4$ msr for the SHMS. For the choice of the kinematics, special attention was taken onto the angular and momentum limits of the spectrometers: for the HMS, $10.5^\circ \leq \theta \leq 85^\circ$ and $1 \leq P_0 \leq 7.3$ GeV/c, and for the SHMS, $5.5^\circ \leq \theta \leq 40^\circ$ and $2 \leq P_0 \leq 11$ GeV/c. In addition, the opening angle between the spectrometers is physically constrained to be larger than 17.5°. The invariant mass W was kept to $W \geq 0.59$ GeV for all settings. The projected uncertainties and A_{zz} are summarized in Table 2, and displayed in Fig. 3.

A total of 14 days of beam time is requested for production data, with an additional 5 days of expected overhead.

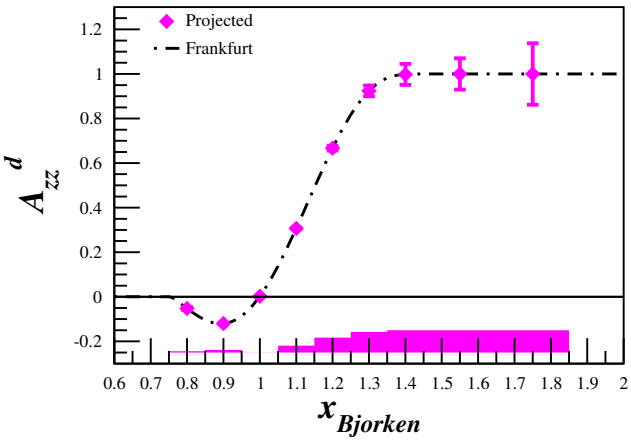

Figure 3: Projected statistical errors for the tensor asymmetry A_{zz} with 14 days of beam time. Data at different Q^2 are combined with an x-binning that varies slightly per point, but is approximately ± 0.05. The band represents the systematic uncertainty. Also shown are the calculations from Frankfurt and Strikman [1].

3.1 Experimental Method

As in the case for E12-13-011, the measured double differential cross section for a spin-1 target characterized by a vector polarization P_z and tensor polarization P_{zz} is expressed as,

$$\frac{d^2\sigma_p}{d\Omega dE'} = \frac{d^2\sigma_u}{d\Omega dE'}\left(1 - P_z P_B A_1 + \frac{1}{2}P_{zz}A_{zz}\right), \tag{1}$$

where, σ_p (σ_u) is the polarized (unpolarized) cross section, P_B is the incident electron beam polarization, and A_1 (A_{zz}) is the vector (tensor) asymmetry of the virtual-photon deuteron cross section. This allows us to write the polarized tensor asymmetry with $0 < P_{zz} \leq 1$ using an unpolarized electron beam as

$$A_{zz} = \frac{2}{P_{zz}}\left(\frac{\sigma_p}{\sigma_u} - 1\right), \tag{2}$$

where σ_p is the polarized cross section. The tensor polarization is given by

$$P_{zz} = \frac{n_+ - 2n_0 + n_-}{n_+ + n_- + n_0}, \tag{3}$$

where n_m represents the population in the $m_z = +1$, -1, or 0 state.

Eq. 2 reveals that the asymmetry A_{zz} compares two different cross sections measured under different polarization conditions of the target: positively tensor polarized and unpolarized. To obtain the relative cross section measurement in the same configuration, the same target cup and material will be used at alternating polarization states (polarized vs. unpolarized), and the magnetic field providing the quantization axis will be oriented along the beamline at all times. This field will always be held at the same value, regardless of the target material polarization state. This process, identical to that used for E12-13-011, ensures that the acceptance remains consistent within the stability (10^{-4}) of the super conducting magnet.

Since many of the factors involved in the cross sections cancel in the ratio, Eq. 2 can be expressed in terms of the charge normalized, efficiency corrected numbers of tensor polarized (N_p) and unpolarized (N_u) counts,

$$A_{zz} \;=\; \frac{2}{f P_{zz}}\left(\frac{N_p}{N_u} - 1\right). \tag{4}$$

The dilution factor f corrects for the presence of unpolarized nuclei in the target and is defined by

$$f = \frac{N_D\sigma_D}{N_N\sigma_N + N_D\sigma_D + \Sigma N_A\sigma_A}, \tag{5}$$

where N_D is the number of deuterium nuclei in the target and σ_D is the corresponding inclusive double differential scattering cross section, N_N is the nitrogen number of scattered nuclei with cross section σ_N, and N_A is the numbers of other scattering nuclei of mass number A with cross section σ_A. The denominator of the dilution factor can be written in terms of the relative volume ratio of ND_3 to LHe in the target cell, otherwise known as the packing fraction p_f. In our case of a

Source	Systematic
Polarimetry	9.0%
Dilution/packing fraction	4.0%
Radiative corrections	1.5%
Charge Determination	1.0%
Detector resolution and efficiency	1.0%
Total	10%

Table 3: Estimates of the scale dependent contributions to the systematic error of A_{zz}.

cylindrical target cell oriented along the magnetic field, the packing fraction is exactly equivalent to the percentage of the cell length filled with ND_3.

The time necessary to achieve the desired precision δA is:

$$T = \frac{N_T}{R_T} = \frac{16}{P_{zz}^2 f^2 \delta A_{zz}^2 R_T} \tag{6}$$

where R_T is the total rate and $N_T = N_p + N_u$ is the total estimated number of counts to achieve the uncertainty δA_{zz}.

3.1.1 Statistical Uncertainty

To investigate the statistical uncertainty we start with the equation for A_{zz} using measured counts for polarized data (N_p) and unpolarized data (N_u),

$$A_{zz} = \frac{2}{f P_{zz}} \left(\frac{N_p}{N_u} - 1 \right). \tag{7}$$

The statistical error with respect to counts is then

$$\delta A_{zz} = \frac{2}{f P_{zz}} \sqrt{\left(\frac{\delta N_p}{N_u} \right)^2 + \left(\frac{N_p \delta N_u}{N_u^2} \right)^2}. \tag{8}$$

3.1.2 Systematic Uncertainty

Table 3 shows a list of the scale dependent uncertainties contributing to the systematic error in A_{zz}.

With careful minimization, the uncertainty in P_z can be held to better than 4%, as demonstrated in the recent g2p/GEp experiment [6]. This leads to a a relative uncertainty in P_{zz} of 7.7%. Alternatively, the tensor asymmetry can be directly extracted from the NMR lineshape as discussed in Sec. **??**, with similar uncertainty. The uncertainty from the dilution factor and packing fraction of the ammonia target contributes at the 4% level. The systematic effect on A_{zz} due to the QED radiative corrections will be quite small. For our measurement there will be no polarized radiative corrections at the lepton vertex, and the unpolarized corrections are known to better than 1.5%.

Charge calibration and detector efficiencies are expected to be known better to 1%, but the impact of time-dependent drifts in these quantities must be carefully controlled.

Time dependent factors

Eq. 4 involves the ratio of counts, which leads to cancellation of several first order systematic effects. However, the fact that the two data sets will not be taken simultaneously leads to a sensitivity to time dependent variations which will need to be carefully monitored and suppressed. To investigate the systematic differences in the time dependent components of the integrated counts, we need to consider the effects from calibration, efficiency, acceptance, and luminosity between the two polarization states.

Fluctuations in luminosity due to target density variation can easily be kept to a minimum by keeping the material beads at the same temperature for both polarization states by control of the microwave and the LHe evaporation. The He vapor pressure reading can give accuracy of material temperature changes at the level of $\sim$0.1%. Beam rastering can also be controlled to a high degree.

The acceptance of each cup can only change as a function of time if the magnetic field changes. The capacity to set and reset and hold, set-ability, the target supper conducting magnet to a desired holding field is $\delta B/B$ =0.01%. This implies that like the cup length l and the acceptance $\mathcal{A}$ for each polarization states is the same.

In order to look at the effect on A_{zz} due to drifts in beam current measurement calibration and detector efficiency we rewrite Eq. 4 explicitly in terms of the raw measured counts N_1 and N,

$$\begin{aligned} A_{zz} &= \frac{2}{fP_{zz}}\left(\frac{N_1^c}{N^c}-1\right) \\ &= \frac{2}{fP_{zz}}\left(\frac{Q\varepsilon l\mathcal{A}}{Q_1\varepsilon_1 l\mathcal{A}}\frac{N^1}{N}-1\right) \end{aligned} \tag{9}$$

where Q represents the accumulated charge, and ε is the detector efficiency. The target length l and acceptance $\mathcal{A}$ are identical in both states to first order.

We can then express Q_1 as the change in beam current measurement calibration that occurs in the time it takes to collect data in one polarization state before switching such that $Q_1 = Q(1-dQ)$. In this notation dQ is a dimensionless ratio of changes in different polarization states. A similar representation is used for drifts in detector efficiency leading to,

$$A_{zz} = \frac{2}{fP_{zz}}\left(\frac{N_1 Q(1-dQ)\varepsilon(1-d\varepsilon)}{NQ\varepsilon}-1\right). \tag{10}$$

which leads to,

$$A_{zz} = \frac{2}{fP_{zz}}\left(\frac{N_1}{N}(1-dQ-d\varepsilon+dQd\varepsilon)-1\right). \tag{11}$$

For estimates of the dQ and $d\varepsilon$ we turn to previous experimental studies. For HRS detector drift during JLab transversity experiment E06-010, the detector response was measured such that the normalized yield for same condition over a three month period indicated little change ($< 1\%$). These measurement where then use to show that for short time (20 minutes periods between target spin flip), the detector drift is estimated to be less than 1% times the ratio of the time period between target spin flip and three months. For the present experiment we use the same estimate except for the period between target polarization states used is $\sim$12 hours leading to an overall

drift $d\varepsilon \sim 0.01\%$. A similar approach can be used to establish an estimate for dQ using studies from the data from the (g2p/GEp) experiment resulting in $d\varepsilon \sim 0.01\%$.

To express A_{zz} in terms of the estimated experimental drifts in efficiency and current measurement we can write,

$$A_{zz} = \frac{2}{fP_{zz}}\left(\frac{N_1}{N} - 1\right) \pm \frac{2}{fP_{zz}}d\xi. \tag{12}$$

This leads to a contribution to A_{zz} on the order of $1 \times 10^{-}3$,

$$dA_{zz}^{drift} = \pm\frac{2}{fP_{zz}}d\xi = \pm 3.7 \times 10^{-3}. \tag{13}$$

Though a very important contribution to the error this value allows a clean measurement of $A_{zz} = 0$ at $x = 0.45$ without overlap with the Hermes error bar. For this estimate we assume only two polarization state changes in a day. If it is possible to increase this rate then the systematic effect in A_{zz} also decreases accordingly.

Naturally detector efficiency can drift for a variety of reasons, for example including fluctuations in gas quality, HV drift or drifts in the spectrometers magnetic field. All of these types of variation as can be realized both during the experiment though monitoring as well as systematic studies of the data collected.

There can be difficult to know changes in luminosity however the identical condition of the two polarization states minimizes the relative changes in time. There are also checks on the consistency of the cross section data that can be use ensuring the quality of each run used in the asymmetry analysis.

4 Summary

References

[1] L. Frankfurt and M. Strikman, Phys.Rept. **160**, 235 (1988).

[2] M. Sargsian, private communication, to be published.

[3] R. A. Gilman and F. Gross, J.Phys. **G28**, R37 (2002).

[4] R. Schiavilla, R. B. Wiringa, S. C. Pieper, and J. Carlson, Phys.Rev.Lett. **98**, 132501 (2007).

[5] P. Bosted and V. Mamyan, (2012).

[6] D. Keller, "Uncertainty in DNP Target Data for E08-007", JLab-TN-051.